

Multifunctional Resistive-Heating and Color-Changing Monofilaments Produced by a Single-Step Coaxial Melt-Spinning Process

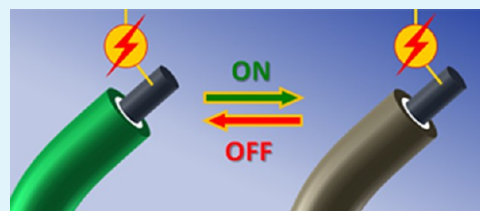
Alexis Laforgue,* Geoffroy Rouget, Sylvain Dubost, Michel F. Champagne, and Lucie Robitaille

National Research Council Canada, 75 De Mortagne Boulevard, Boucherville, Québec J4B 6Y4, Canada

S Supporting Information

ABSTRACT: Multifunctional coaxial monofilaments were successfully produced by melt-spinning several polymer composites in a single-step. The external layer of the monofilaments was a thermochromic composite having a color-transition at 40 °C (above the ambient temperature) in order to avoid control interferences by the external temperature. The core layer of the monofilaments was a conductive polymer nanocomposite whose resistive heating properties were used to control the monofilament's temperature and therefore its color using electrical current. The careful selection of the materials and adequate formulation allowed to obtain a trilayer structure with enhanced compatibility between the layers. The mechanical properties of the monofilaments were improved by a solid-state stretching step while also decreasing their diameter. A 64 cm² prototype fabric was woven to characterize the resistive-heating and color-changing properties of the monofilaments. Exceptional thermal output levels were reached, with a temperature rising up to over 100 °C at voltages above 110 V. The reversible color change properties were also successfully demonstrated.

KEYWORDS: monofilament, melt-spinning, multifunctional, electrochromic, color change, resistive heating, coaxial monofilament, smart textile



1. INTRODUCTION

The textile industry is currently moving toward more and more sophisticated applications with the addition of very specific high-end functionalities, such as health monitoring,^{1–3} performance monitoring,^{4,5} temperature control,^{6–8} electronics,^{9–14} electroluminescence,¹⁵ flexible photovoltaics,¹⁶ energy storage,^{17–19} etc. Most of the current so-called “smart textiles” are made of technologies being integrated into existing textile supports rather than made of truly functional monofilaments. Nevertheless, a number of functional monofilaments have been developed, which respond to diverse environmental changes such as temperature^{6,20–23} or humidity.^{24,25} These monofilaments represent a significant first step toward the development of intelligent monofilaments and textiles.

One of the most striking changes in a textile property is the alteration of its color, and a number of smart textile technologies have been developed toward this aim.^{20,26–29} Among them, the use of thermochromic dyes that undergo a color change at a specific temperature has been particularly exploited.^{20,30–33} Thinking further, some researchers as well as artists have designed systems in which the color change is controlled by the support temperature rather than the ambient temperature, allowing to trigger the transition to a certain extent. The work of Joanna Berzowska provides a good example of textiles incorporating color-changing elements (applied using a thermochromic ink) where the color change is caused by the resistive heating of an electrically conductive yarn woven or embroidered into the fabric.³⁰ The limitation of this work is

that the textile only heats-up at the immediate proximity of the conductive yarns, meaning that an additional conductive thread has to be woven or embroidered in the textile to trigger the color-change. In a recent work, we investigated color changing textiles where the whole textile is being conductive, allowing one to draw any feature (letters, logos, etc..) with a thermochromic ink anywhere on the textile. When a current was passed through the textile, the entire thermochromic feature underwent a color change.³⁴ However, this textile still suffered from non-negligible limitations: the current was passed through the whole textile, raising obvious safety considerations.

In the present work, we investigated the incorporation of a controllable color-change functionality, directly and entirely within the monofilament, rather than applying functional materials to an existing textile. This is a new step toward truly intelligent textiles. The idea was to produce a coaxial multilayer monofilament whose core layer could be electrically actionable to trigger the color change of the external layer (cf. Figure 1). Some examples following the idea of functional coaxial monofilaments have already been proposed,^{19,35–37} but only few of them have been truly demonstrated.^{26,38–40}

The monofilament was produced using pilot-scale monofilament melt-spinning and solid-state poststretching equipments and fully characterized. A multimonomilament prototype was

Received: March 19, 2012

Accepted: May 31, 2012

Published: May 31, 2012

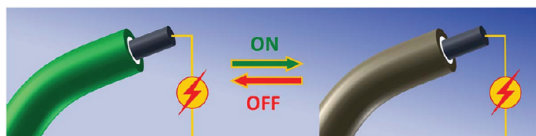


Figure 1. Scheme of principle of a coaxial multilayer monofilament whose conductive core can be used to reversibly trigger the color-change of the external layer.

woven and its electrothermic and color-change properties demonstrated.

2. MATERIALS AND METHODS

Materials. A masterbatch of polypropylene (PP) filled with 20 wt % multiwalled carbon nanotubes (Fibril MB3020–01) was supplied by Hyperion Catalysis (USA). A monofilament grade low melting temperature PP copolymer (DS6D21) was purchased from Dow (Melting temp. 142 °C; MFI 230 °C/2.16 kg: 8 g/10 min). A white masterbatch of PP containing 50 wt % of TiO₂ was supplied by Standridge (grade 4837). Custom made masterbatches of PP containing 25 wt % thermochromic microcapsules (TCM) having a color transition at 40 °C were purchased from LCR Hallcrest.

Processing. The PP-MWNT masterbatch was diluted to a MWNT content of 12.5 wt % on a Werner & Pfleiderer twin-screw extruder using the Dow PP. All other formulations were done on the single-screw extruders of the multilayer melt-spinning line.

Multilayer monofilaments were produced using a Randcastle coextrusion line equipped with a specially designed single-hole die (diameter: 1 mm) allowing the extrusion of filaments having up to three coaxial layers made of three different materials (see Figure S11 in the Supporting Information). The extrusion temperatures of the core layer (PP-MWNT), intermediate layer (PP-TiO₂) and sheath layer (PP-TCM-TiO₂) were set to 220, 210, and 165 °C, respectively. The screw rotation speeds were set to 15 rpm, 7.5 and 7.5 rpm for the core, intermediate, and sheath layers, respectively, in order to maximize the core layer relative thickness. The monofilaments were collected on a spool with minimal stretching.

The extruded monofilaments were poststretched at 130 °C using a pilot scale stretching line (Monofilament Extrusion Technologies, UK) including a temperature conditioning water bath, a slow haul-off (SHO) unit, a 8 ft long convection oven, a fast haul-off (FHO) unit and a winding unit (see Figure S12 in the Supporting Information). The monofilament stretching ratio was controlled by the speed ratio between the SHO and FHO units.

Characterization. The mechanical properties were investigated using an Instron 55R1123 tensile tester under controlled conditions (23 °C, 50% relative humidity) with a 1 kN cell and at a speed of 10 mm/min. Five samples were tested for each condition and the results displayed are average values and corresponding standard deviations.

The optical microscopy was performed on a Leitz Dialux 20 microscope equipped with a computer interfaced digital camera.

Thermal imaging was carried out with a ThermaCAM SC620 camera and recorded using the software ThermaCAM Researcher Pro 2.9 (FLIR Systems AB).

The electrical properties were investigated by connecting the prototype fabric to a potentiometer plugged to the mains.

3. RESULTS AND DISCUSSION

Formulation. The conductive core layer of the monofilament was composed of polypropylene (PP) incorporating 12.5 wt % of multiwalled carbon nanotubes (MWNTs). It was obtained by the melt-dilution of a commercial masterbatch from Hyperion Catalysis having a MWNT content of 20 wt %. The polymer used for the dilution was a PP copolymer of monofilament grade (DS6D21 from Dow), to impart monofilament-forming properties to the composite. The MWNT content was selected from a previous study.³⁹ The conductivity



Figure 2. Photographs of 100 μm thick hot-pressed films of green-to-colorless TCM-PP composites with different TCM contents. (a) 10 wt %; (b) 15 wt %; (c) 20 wt %.

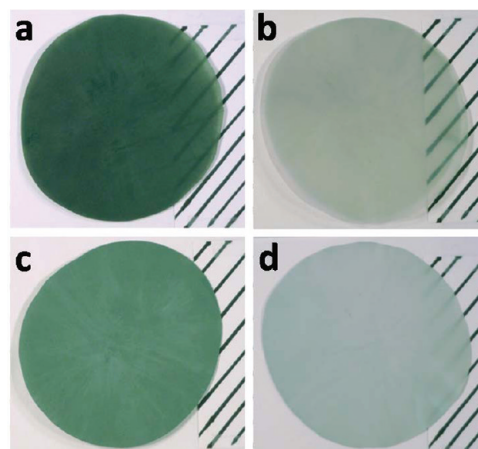


Figure 3. Photographs of 100 μm thick films of green-to-white TCM-PP composites, (a, b) without or (c, d) with 1 wt % TiO₂ content, (a, c) below and (b, d) above the color transition temperature. TCM content in the composite: 15 wt %.

of the core layer was ca. 1 S/cm for as-spun (unstretched) monofilaments, which is adequate to impart resistive heating properties to the material.

A formulation study was performed for the sheath layer material. Masterbatches of PP containing thermochromic microcapsules (TCM) were custom produced by LCR Hallcrest. The TCMs had a transition temperature of 40 °C in order to hinder any color transition caused by an environmental condition change. The content of microcapsules was varied from 10 to 20 wt % by melt-diluting the masterbatch with the DS6D21 PP. Figure 2 presents the photographs of 100 μm thick hot-pressed films of TCM-PP composites with different TCM contents. No significant color bleaching was observed by diluting from 20 to 15 wt %, but diluting further proved to be detrimental to the color intensity. A TCM content of 15 wt % was then selected for the rest of the study.

TCMs always change from a colored state at low temperature to a transparent state at high temperature.^{20,41} TCM



Figure 4. Spools of a green-to-beige trilayer coaxial monofilament after melt-spinning (left) and after solid-state poststretching at a ratio $\lambda = 7$ (right).

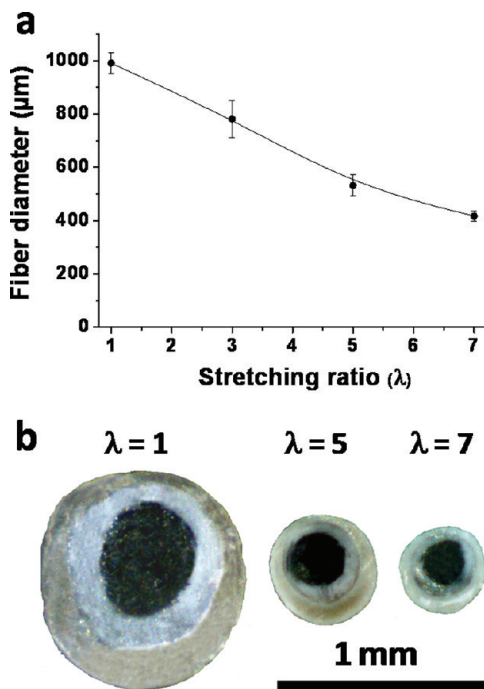


Figure 5. (a) Variation of the monofilament diameter with stretching ratio. (b) Cross-section images of a trilayer monofilament before and after solid-state poststretching at different ratios.

composites can undergo color-to-color transitions if additional dyes are being incorporated into the composite, but always from a dark state (cold) to clear state (hot). In the case of a coaxial monofilament having a black core-layer, this transparency can be a severe limitation in the color-to-color contrast. To impart some opacity to the external layer material, we incorporated titanium dioxide (TiO_2) into the composite. TiO_2 is commonly used as a white dye in numerous industries including plastics and painting applications. Very low contents are sufficient to efficiently whiten materials. Figure 3 shows the different color states of green-to-colorless TCM-PP composites. A significant transparency of the TCM-PP composites was observed, especially at the hot clear state (cf. Figure 3b). On the other hand, the composite having a TiO_2 content of 1 wt % was efficiently rendered opaque. The composition for the

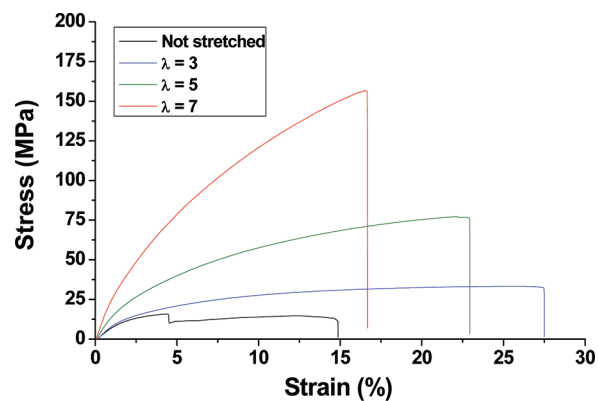


Figure 6. Typical stress–strain curves of the trilayer monofilaments after extrusion and at different stretching ratios.

sheath layer was thus selected to be a PP composite with 15 wt % TCMs and 1 wt % TiO_2 .

Monofilament Processing and Characterization. The concept developed in this project was the combination of a

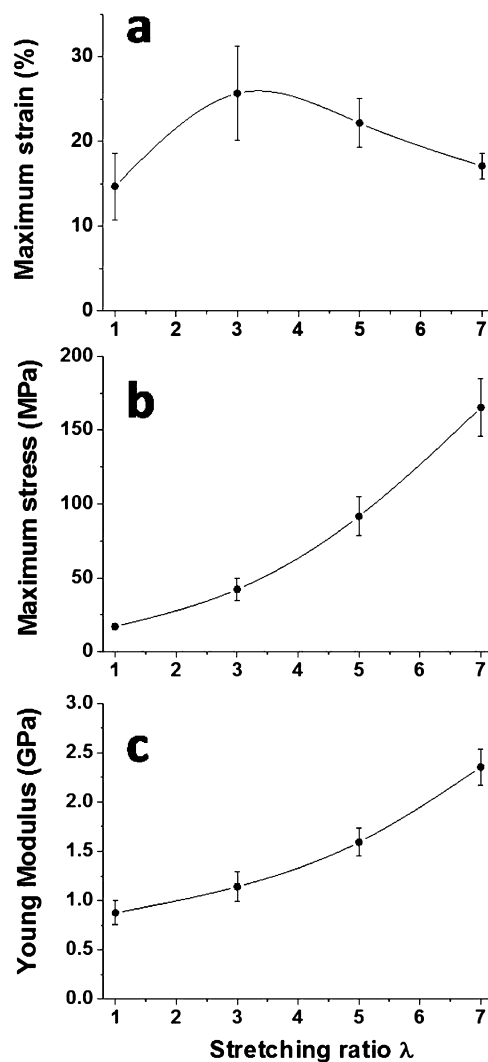


Figure 7. Mechanical properties of the monofilaments at different stretching ratios (extracted from the stress–strain curves). (a) Maximum strain ; (b) monofilament tenacity (maximum stress); (c) Young modulus.

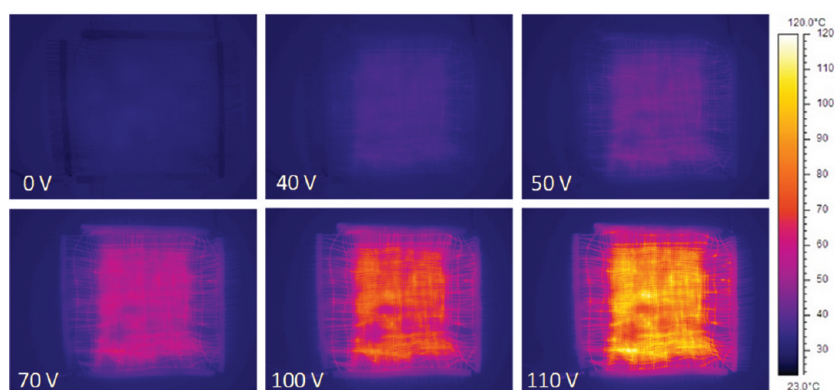


Figure 8. Infrared camera images of the 64 cm² fabric prototype at different applied voltages.

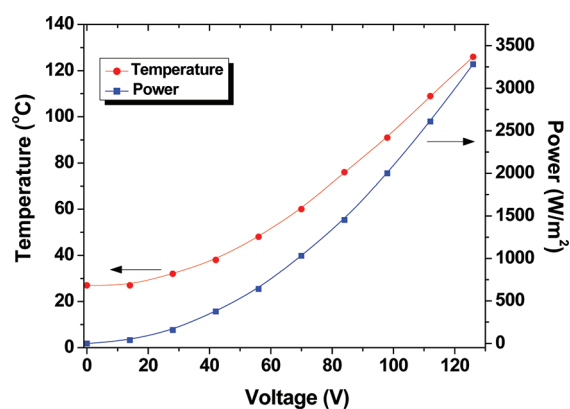


Figure 9. Temperature and thermal power output of the textile prototype as a function of applied voltage.

conductive core layer, whose resistive properties heating (Joule effect) could be used to trigger the color change of a thermochromic upper layer. The simplest configuration required for this purpose would be a two-layers coaxial monofilament. However, spin-line instabilities as well as irregularities at the layers interface were observed during the monofilaments melt-spinning, due to chemical incompatibilities between the two composites. It was then decided to add an intermediate layer made of the same PP used to melt-dilute both composites. Moreover, to improve the upper layers' opacity toward the black core, we incorporated 10 wt % TiO₂ into the intermediate layer. It proved to efficiently compatibilize the core and external layers while allowing us to fully hide the core layer. The thickness of each layer could be controlled by the screw rate ratio of the layer's respective extruders.³⁹

After production, the monofilaments were stretched at different ratios using a pilot-scale poststretching line (see Experimental Section and Figure S12 in the Supporting Information), at a temperature below the crystalline melting point of the composites (130 °C), in order to decrease their diameter and improve their mechanical properties by causing a controlled crystallization of the polymer.⁴² The ratio was determined by the difference between the rolling speeds the haul-off units located on each side of the oven. Figure 4 shows spools of a green-to-beige trilayer coaxial monofilament after melt-spinning (left) and after having been poststretched at a ratio $\lambda = 7$ (right). The diameter was progressively decreased from 1 mm after extrusion to ca. 400 μm after stretching to ratio of 7, as can be observed in Figure 5a. The coaxiality of the

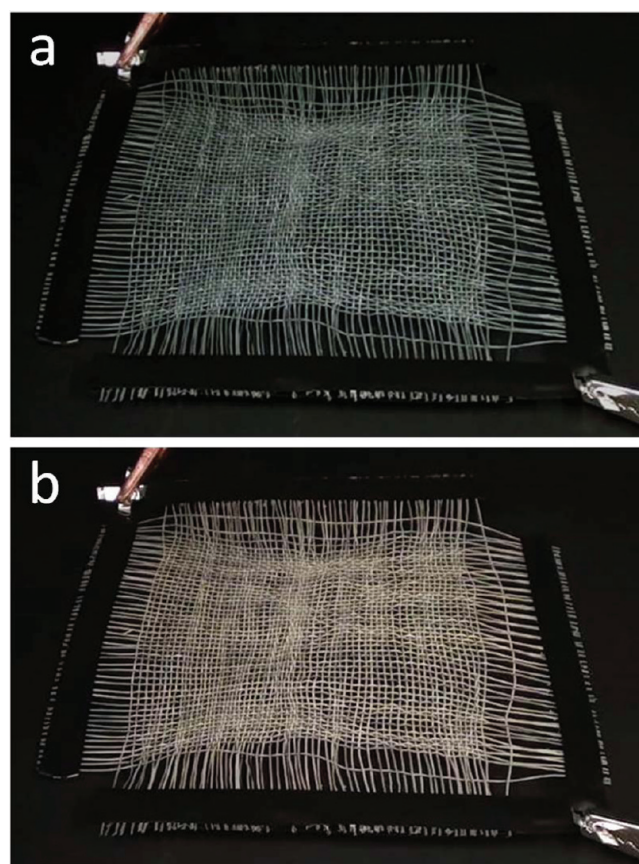


Figure 10. Textile prototype (a) in its cold color (0 V, ambient temperature) and (b) in its hot color (60 V, 50 °C).

layers was well preserved during the stretching process (see Figure 5b).

The conductivity of the core layer was found to decrease with the solid-state stretching ratio from 1 S/cm for the as-spun monofilament to 1×10^{-2} S/cm at $\lambda = 7$.³⁹ This was due to a progressive loss of electrical percolation in the composite due to an anisotropic disentanglement and alignment of the MWNTs in the stretching direction and the resulting isolation of the MWNT agglomerates by nonconductive polymer phases. This phenomenon has already been observed for carbon nanotubes-polymer composites^{43–45} and can be circumvented to some extent by subsequent heat annealing treatments.^{46–48} However, the range of conductivity for solid-stretched monofilaments being still adequate for resistive heating

applications, postannealing treatments were not investigated in this study.

The mechanical properties of the monofilaments were characterized using traction experiments. Typical stress–strain curves are presented in Figure 6 and the resulting mechanical properties, plotted in Figure 7. The as-spun monofilaments presented two steps of fracture, corresponding to the different layers, the core layer being stiffer and breaking at ca. 5% followed by the break of the external layers. This result showed that the interface between the layers was weak. After stretching, no such multistep fracture was observed, suggesting that the stretching process improved the adhesion between the layers.

A further indication of an interlayer cohesion improvement upon stretching is the observed increase in maximum strain from ca. 15% for the as-spun monofilament to ca. 25% for the monofilament stretched at a ratio of 3 (cf. Figure 7a). We previously showed that the poststretching of the sole core layer did not improve its maximum strain.³⁹ It is thus believed that the increase in maximum strain was caused by an improved cohesion between the layers and a consequent better distribution of the stress among the three layers, which can then sustain more deformation. For a stretching ratio higher than 3, the maximum strain was then progressively decreased, possibly because of an effective orientation and crystallization of the PP chains leading to an increased stiffness of the composite, as evidenced by the significant increase in tenacity and Young modulus (see Figure 7b,c, respectively). The tenacity of the monofilaments was increased by nearly an order of magnitude after stretching at a ratio of 7, resulting in monofilaments having enough mechanical properties to be woven using industrial machines.

Prototype Fabrication and Characterization. A 64 cm² prototype textile consisting of 130 stretched monofilaments ($\lambda = 7$) was woven using a manual weaving loom. The two upper layers of each monofilament were then selectively stripped off at the extremities and the core layer of each monofilament was connected to an aluminum strip using silver epoxy. All monofilaments were connected in a parallel configuration, in order to decrease the ohmic resistance of the overall electric circuit. The textile was then connected to a power source to test its resistive heating properties.

Figure 8 presents infrared optical images of the textile at different applied voltages. The prototype was able to heat-up efficiently and evenly when a current was passed through the core layer. The temperature of a virtual point located at the center of the textile was then monitored as a function of voltage (see Figure 9). Not much temperature increase was detected below 20 V, thanks to an efficient current flow in the PP-MWNT composite. Above 20 V, the temperature began to rise following the voltage increase and reached over 120 °C at 120 V. This impressive temperature increase was obtained thanks to the exceptional electric and thermal conductivity of carbon nanotubes.^{49–51} The thermal power output reached over 3000 W/m² at 120 V, an order of magnitude higher than the commercially available resistive heating textiles obtained by coating conducting polymer layers on textile substrates.^{52–54} When the temperature reached the transition temperature of the TCMs located in the external layer (i.e., 40 °C), the color of the fabric turned from green to beige, as can be observed in Figure 10 and video file SI4 in the Supporting Information. When the voltage was turned off, the temperature decreased and the fabric progressively turned back to its original green color. The process could be repeated numerous times with no

loss of color reversibility. The green-to-beige (cold-to-hot) transition time could be varied from 30 to 2 s, according to the amount of power applied (see Figure SI3 in the Supporting Information). However, the beige-to-green (hot-to-cold) transition was controlled by the heat dissipation of the material and was typically between 7 and 20 s.

4. CONCLUSIONS AND PERSPECTIVES

The one-step production of multifunctional monofilaments was successfully achieved through the coaxial melt-spinning of materials having different properties. The careful selection of the materials and adequate formulation allowed to obtain a trilayer structure with enhanced compatibility between the layers. The mechanical properties of the monofilaments were improved by a solid-state stretching step, which also allowed to decrease their diameter. A prototype fabric was woven and tested. The temperature and color of the fabric proved to be reversibly controllable, according to the amount of current passed through the conductive core of the monofilaments. Exceptional thermal output levels were reached by the monofilaments, with a temperature rising up to over 100 °C at voltages above 110 V. The cold-to-hot color transition time of the fabric could be controlled (from 2 to 30 s) by tuning the power applied to the fabric.

These resistive heating/color-changing monofilaments could find applications and numerous fields including active visual camouflage, dynamic mural textiles, heating textiles having a visual temperature state indication, fashion clothing and accessories, etc.

The main limitation of the monofilaments was the important power needed to induce the color change (~ 500 W/m²). This is due to the conductivity of the core nanocomposite material ($\sim 1 \times 10^{-2}$ S/cm), which was still too low for an efficient energy transport within long monofilaments. This could be possibly improved by formulation and postprocess fine-tuning.^{46,48} These studies as well as the incorporation of the functional monofilaments into conventional textiles are part of future developments of the technology.

■ ASSOCIATED CONTENT

Supporting Information

photographs and descriptions of the pilot-scale equipment used to produce and poststretch the monofilaments, graph representing the cold-to-hot color transition time according to the power applied and video representing the fabric's reversible color transition. This material is available free of charge via the Internet at <http://pubs.acs.org/>.

■ AUTHOR INFORMATION

Corresponding Author

*E-mail: alexis.laforgue@cnrc-nrc.gc.ca.

Notes

The authors declare no competing financial interest.

■ ACKNOWLEDGMENTS

The authors acknowledge Robert Lemieux, François Vachon, Jacques Dufour, Manon Plourde, and Karine Théberge from NRC-Boucherville, for their respective technical participation to the experiments.

REFERENCES

- (1) Carpi, F.; De Rossi, D. *IEEE Trans. Inform. Technol. Biomed.* **2005**, *9* (3), 295–318.
- (2) Catrysse, M.; Puers, R.; Hertleer, C.; Langenhove, L. V.; Egmond, H. v.; Matthys, D. *Sens. Actuators, A* **2004**, *114*, 302–311.
- (3) Loriga, G.; Taccini, N.; Pacelli, M.; Paradiso, R. *IEEE Ind. Electron. Mag.* **2007**, Fall, 5–8.
- (4) Under Armour. <http://www.underarmour.com/e39>
- (5) Textronics, Inc. <http://www.textronicsinc.com/>
- (6) Outlast Technologies, Inc. <http://www.outlast.com/>
- (7) WarmX. <http://www.warmx.de/>
- (8) Gerbing's Heated Clothing. <http://gerbing.eu>
- (9) Berzowska, J. *Textile* **2005**, *3* (1), 2–19.
- (10) Buechley, L.; Eisenberg, M. *Pers. Ubiquit. Comput.* **2009**, *13*, 133–150.
- (11) Cherenack, K.; Zysset, C.; Kinkeldei, T.; Münzenrieder, N.; Tröster, G. *Adv. Mater.* **2010**, *22*, 5178–5182.
- (12) Gould, P. *Mater. Today* **2003**, 38–43.
- (13) Hamed, M.; Forchheimer, R.; Inganäs, O. *Nat. Mater.* **2007**, *6*, 357–362.
- (14) Jung, S.; Lauterbach, C.; Strasser, M.; Weber, W. *IEEE Int. Solid-State Circuit Conf.* **2003**, 386–387.
- (15) Hu, B.; Li, D.; Manandhar, P.; Fan, Q.; Kasilingam, D.; Calvert, P. *J. Mater. Chem.* **2012**, *22*, 1598–1605.
- (16) Krebs, F. C.; Biancardo, M.; Winther-Jensen, B.; Spanggaard, H.; Alstrup, J. *Sol. Energy Mater. Sol. Cells* **2006**, *90*, 1058–1067.
- (17) Gu, J. F.; Gorgutsa, S.; Skorobogatiy, M. *Smart Mater. Struct.* **2010**, *19*, 115006.
- (18) Laforgue, A. *J. Power Sources* **2011**, *196*, 559–564.
- (19) Service, R. F. *Science* **2003**, *301*, 909–911.
- (20) Christie, R. M.; Robertson, S.; Taylor, S. *Colour: Design and Creativity* **2007**, *1* (5), 1–11.
- (21) Gao, X.-y.; Han, N.; Zhang, X.-x.; Yu, W.-y. *J. Mater. Sci.* **2009**, *44*, 5877–5884.
- (22) Mengjin, J.; Xiaoqing, S.; Jianjun, X.; Guangdou, Y. *Sol. Energy Mater. Sol. Cells* **2008**, *92*, 1657–1660.
- (23) Zhang, X. X. *J. Mater. Sci.* **2005**, *40*, 3729–3734.
- (24) Devaux, E.; Aubry, C.; Campagne, C.; Rochery, M. *J. Eng. Fibers Fabr.* **2011**, *6* (3), 13–24.
- (25) Dhinojwala, A.; Blackledge, T.; Agnarsson, I. International Patent WO 2009/135161, 2009.
- (26) Gauvreau, B.; Guo, N.; Schicker, K.; Stoeffler, K.; Boismenu, F.; Aji, A.; Wingfield, R.; Dubois, C.; Skorobogatiy, M. *Opt. Express* **2008**, *16* (20), 15677–15693.
- (27) Invernale, M. A.; Ding, Y.; Sotzing, G. A. *ACS Appl. Mater. Interfaces* **2010**, *2*, 296–300.
- (28) Peng, H.; Sun, X.; Cai, F.; Chen, X.; Zhu, Y.; Liao, G.; Chen, D.; Li, Q.; Lu, Y.; Zhu, Y.; Jia, Q. *Nat. Nanotechnol.* **2009**, *4*, 738–741.
- (29) Wakita, A.; Shibutani, M. *Proceedings of the 2006 ACM SIGCHI International Conference on Advances in Computer Entertainment Technology*; Association for Computing Machinery: New York, 2006; pp 48–54.
- (30) Berzowska, J.; Bromley, M. *Proceedings of the International Foundation of Fashion Technology Institutes Conference 2007 Extreme Fashion: Pushing the Boundaries of Design, Business and Technology*; Toronto, CA, April 12–15, 2007; International Foundation of Fashion Technology Institutes: New Delhi, India, 2007; pp 1–12.
- (31) Carlyle, T.; Rivera, M. International Patent WO 03/035948, 2003.
- (32) Ono, Y.; Ishimura, N.; Shibahashi, Y. U.S. Patent 2002/0090510, 2002.
- (33) Rubacha, M. *Polym. Adv. Technol.* **2007**, *18*, 323–328.
- (34) Laforgue, A. *J. Mater. Chem.* **2010**, *20*, 8233–8235.
- (35) Baumberg, I.; Berezin, O.; Gorelik, B.; Voskoboinik, M. International Patent WO 2007/004223, 2007.
- (36) Duggal, A. R.; Olson, D. R. U.S. Patent 2004/0212301, 2004.
- (37) Wilderbeek, J. T.; Burdinski, D.; Den Toonder, J. M.; Krans, J. M.; Van Bruggen, M. P. International Patent WO 2005/096075, 2005.
- (38) Chittibabu, K.; Eckert, R. D.; Gaudiana, R.; Li, L.; Montello, A.; Montello, E.; Worsmer, P. International Patent WO 2007/047190, 2007.
- (39) Laforgue, A.; Champagne, M. F.; Dumas, J.; Robitaille, L. *J. Eng. Fibers Fabr.* **2012**, *7* (3), in press.
- (40) Lee, M. R.; Eckert, R. D.; Forberich, K.; Dennl, G.; Brabec, C. J.; Gaudiana, R. A. *Science* **2009**, *324*, 232–235.
- (41) Seeboth, A.; Ruhmann, R.; Mühlhng, O. *Materials* **2010**, *3*, 5143–5168.
- (42) Hu, X.; Alcock, B.; Loos, J. *Polymer* **2006**, *47*, 2156–2162.
- (43) Straat, M.; Toll, S.; Boldizar, A.; Rigdahl, M.; Hagstrom, B. *J. Appl. Polym. Sci.* **2011**, *119*, 3264–3272.
- (44) Deng, H.; Zhang, R.; Bilotti, E.; Loos, J.; Peijs, T. *J. Appl. Polym. Sci.* **2009**, *113*, 742–751.
- (45) Pötschke, P.; Brüning, H.; Janke, A.; Fischer, D.; Jehnichen, D. *Polymer* **2005**, *46*, 10355–10363.
- (46) Straat, M.; Rigdahl, M.; Hagstrom, B. *J. Appl. Polym. Sci.* **2012**, *123*, 936–943.
- (47) Deng, H.; Zhang, R.; Reynolds, C. T.; Bilotti, E.; Peijs, T. *Macromol. Mater. Eng.* **2009**, *294*, 749–755.
- (48) Deng, H.; Skipa, T.; Bilotti, E.; Zhang, R.; Lellinger, D.; Mezzo, L.; Fu, Q.; Alig, I.; Peijs, T. *Adv. Funct. Mat.* **2010**, *20*, 1424–1432.
- (49) Du, J.-H.; Bai, J.; Cheng, H.-M. *Express Polym. Lett.* **2007**, *1* (5), 253–273.
- (50) Liu, K.; Sun, Y.; Lin, X.; Zhou, R.; Wang, J.; Fan, S.; Jiang, K. *ACS Nano* **2010**, *4* (10), 5827–5834.
- (51) Moniruzzaman, M.; Winey, K. I. *Macromolecules* **2006**, *39* (16), 5194–5205.
- (52) Hakansson, E.; Kaynak, A.; Lin, T.; Nahavandi, S.; Jones, T.; Hu, E. *Synth. Met.* **2004**, *144*, 21–28.
- (53) Kaynak, A.; Hakansson, E. *Adv. Polym. Technol.* **2005**, *24* (3), 194–207.
- (54) Sparavigna, A. C.; Florio, L.; Avloni, J.; Henn, A. *Mater. Sci. Appl.* **2010**, *1*, 253–259.